$A(Q)$ at low Q in ed elastic scattering

J.-P. Chen,[1] E. Chudakov,[1] M. Epstein,[2] R. Gilman (contact person),[1,3] C. Glashausser,[3] D.W. Higinbotham (spokesperson),[1] X. Jiang (spokesperson),[3] D.J. Margaziotis,[2] S. Nanda,[1] B. Norum,[4] R. Ransome,[3] B. Reitz,[1] A. Saha,[1] A.J. Sarty,[5] S. Strauch,[6] P. Ulmer,[7] K. Wang,[4] and *the Hall A Collaboration*

[1] *Thomas Jefferson National Accelerator Laboratory, Newport News, Virginia 23606*
[2] *California State University, Los Angeles, CA 90032*
[3] *Rutgers University, Piscataway, New Jersey 08855*
[4] *University of Virginia, Charlottesville, VA 22904*
[5] *St. Mary's University, Halifax, Nova Scotia, CANADA B3H 3C3*
[6] *George Washington University, Washington, DC 20052*
[7] *Old Dominion University Norfolk, VA 23529*

This is an update jeopardy proposal for experiment E02-004, *$A(Q)$ at low Q in ed elastic scattering*. The experimental goal of E02-004 is a very precise, definitive measurement of $A(Q)$, $Q \equiv \sqrt{Q^2}$, at low Q. We aim to improve upon and resolve a discrepancy between two precise older measurements.

These new data will provide a test of models of the deuteron structure, including chiral perturbation theory, and conventional non-relativistic and relativistic models. The currently existing low Q data appear more similar to incomplete Hamiltonian-form relativistic calculations than to complete calculations that overall better describe the full deuteron elastic form factor data set. The data are not of sufficient precision to clearly distinguish what is the sign of the leading-order relativistic corrections. Given this situation, a new attempt at a higher precision measurement of $A(Q)$ was justified, and the January 2002 PAC approved the proposal with B^+ priority.

In this update, we reiterate our interest in the physics motivation. The experimental details are given, including developments since the experiment was initially approved. These developments include an updated uncertainty analysis, reflecting improved systematics obtained in recent experiments, progress on the beam calorimeter needed for the experiment, and a revised run plan and time request. Our beam time request is for six days of beam time to measure the ed elastic scattering $A(Q)$ structure function at low Q. An $\approx$2 – 3 % absolute, $\approx$0.5 – 1.0 % relative $d(e,e')d$ cross section measurement is feasible in Hall A.

INTRODUCTION

In the past decade, our understanding of the elastic deuteron structure has advanced due both to a wide variety of theoretical work and to a few key experiments. The foundation of microscopic calculations is nucleon-nucleon scattering; modern potentials derived during the 1990's have a nearly ideal description of the nucleon-nucleon force, with a reduced χ^2 of about 1 for a pruned nucleon-nucleon data base [1]. The deuteron structure has recently been calculated in several different formulations, but not all of these calculations are at the same level of theoretical maturity.

Much of the recent effort has focused on large momentum transfer scattering. The two key experiments, both performed at Jefferson Lab, were the measurements of the recoil tensor polarization t_{20} to four momentum transfers of $Q^2 = 1.7$ GeV^2 [2] and of the structure function A to $Q^2 = 6.0$ GeV^2 [3]. Comparison of these results to theory has shown that the deuteron structure can be explained with conventional hadronic theories; simple quark models do not predict the data well.

Figure 1 provides a summary of this conventional view of the deuteron structure. There are a number of theoretical calculations, described in more detail below, which provide an excellent description of t_{20}. The structure function A can be described well, to 20 - 30 %, as it falls about eight orders of magnitude. Differences of ≈10 %, which exist between the Jefferson Lab Hall A [3] and Hall C [4] data, are nearly invisible in this plot, and the slight systematic differences between some of the t_{20} data sets also do not seem to be very important. (Complete sets of references to the data, and further discussion on these issues, can be found in recent fits [5] and reviews by Garçon and Van Orden [6], by Sick [7], and by Gilman and Gross [8].) From this overview, it appears that the main theoretical difficulty is then having good control on the minimum of the structure function B, which theoretically results from delicate cancellations and experimentally is not well determined.

In this proposal, we focus on an issue that is hidden by the semi-logarithmic scale of the plots, the status of the structure function A at low momentum transfer. For low energy and momentum transfers, there has been enormous progress in the last several years on a description of the nucleon-nucleon system and the deuteron using both pionless effective field theory (EFT) and chiral perturbation theory (χPT); these approaches may be considered to be firmly tied to quantum chromodynamics (QCD). Quantitative agreement between the theory and data is now possible. But, as we shall show below, an ≈8% discrepancy between the high (<2 %) precision Mainz [9] and Saclay [10] data sets for Q about 0.2 - 0.4 GeV [1] makes the comparison between experiment and theory difficult. This difference may appear small and unimportant, but, to put it in perspective, a 10% uncertainty in A in a region in which its magnitude is 10^{-1} - 10^{-2} is much greater than a 100% uncertainty in B in a region in which its magnitude is 10^{-8}.

A natural experimental bias is to discount the highest Q^2 Mainz data points. However, we argue that the best conventional theory favors the Mainz data over the Saclay data. If indeed the Mainz data are more nearly correct, a few of the theories provide a reasonable description of *all* of the deuteron elastic scattering data, while if the Saclay data are more nearly correct, *no* conventional theory provides a precise description of all of the data.

Thus, with an increasing variety of theoretical approaches, and with the improved theoretical precision of recent years, the discrepancy between the Saclay and Mainz data sets

[1] We use $Q = \sqrt{Q^2}$ throughout this proposal; $Q \neq |\vec{q}|$.

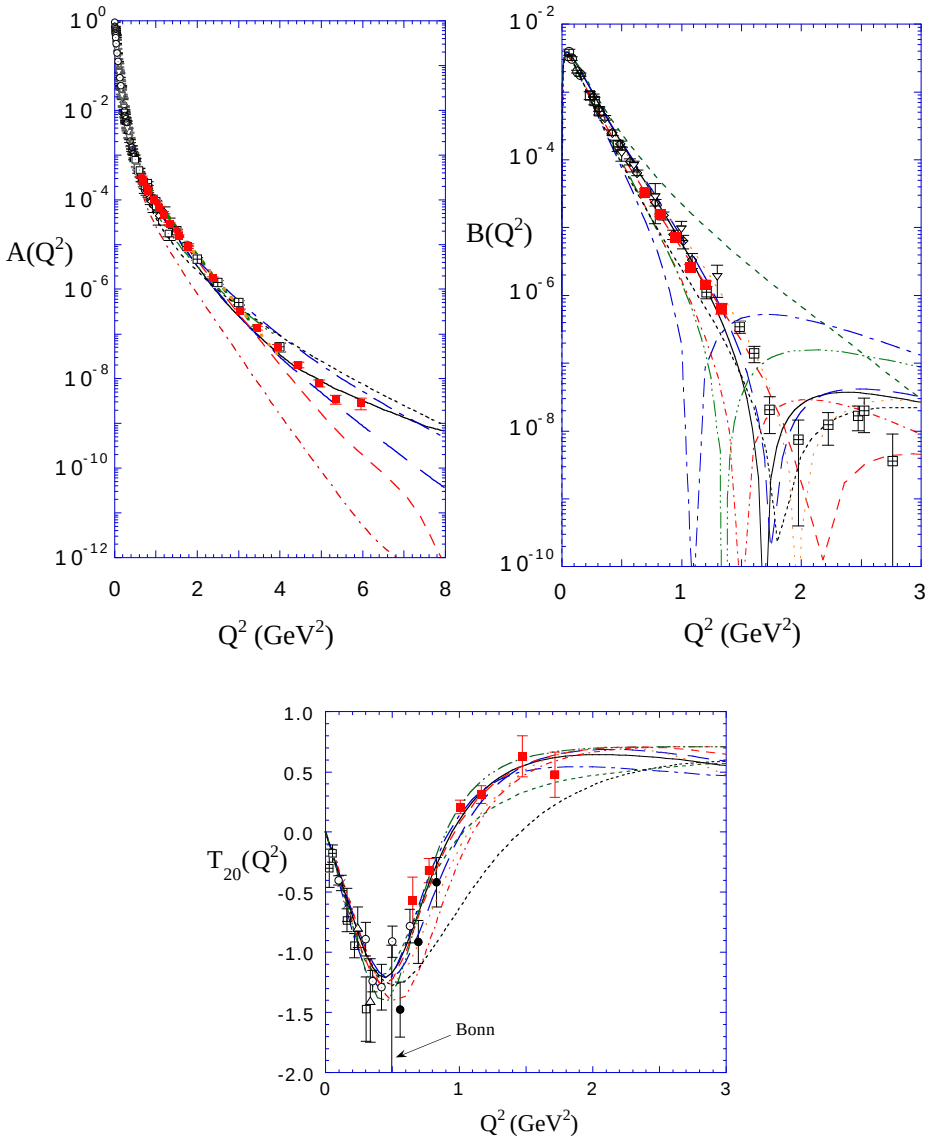

FIG. 1: Experimental data for A, B, and t_{20} compared to eight calculations. The calculations, in order of the Q^2 of their mimima in B, are: CK (long dot-dashed line), PWM (dashed double-dotted line), AKP (short dot-dashed line), VOG full calculation (solid line), VOG in RIA (long dashed line), LPS (dotted line), DB (widely spaced dotted line), FSR (medium dashed line), and ARW (short dashed line). See text for details.

has become an important issue that needs to be resolved. Experimentally, data rates are high, and the experiment can be done in Hall A with only six days of beam time. The main experimental issues include maintaining a good control of systematics and being able to prove the correctness of the results, as they are likely to disagree with one of the existing high precision data sets.

In the following sections, we thoroughly review the motivation for the experiment and

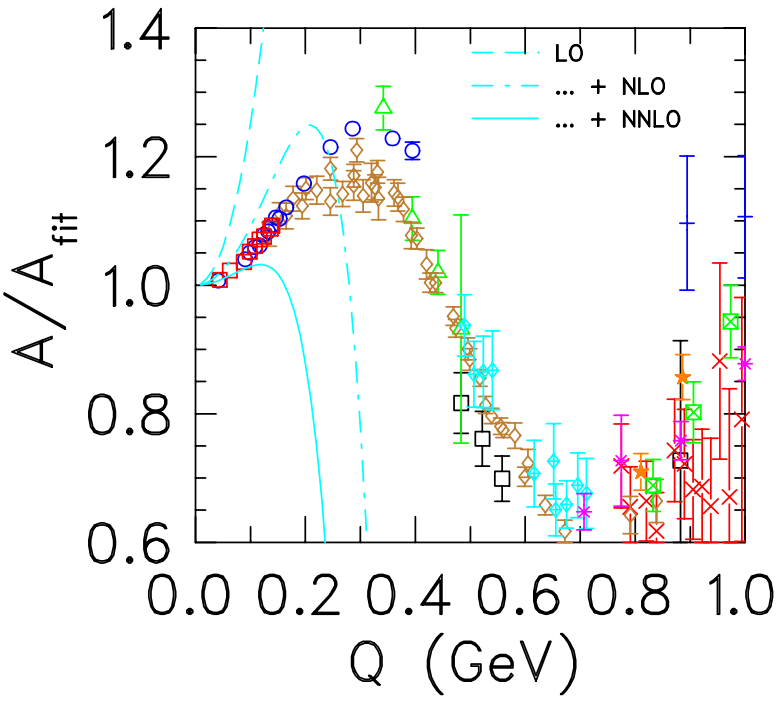

FIG. 2: The data for A at low and moderate Q, divided by a fit function described in the text. The data sets are described in Table I. The $\not\pi$EFT calculations are described in the text.

the experimental details.

DETAILED MOTIVATION

In the one-photon exchange approximation [11] elastic scattering from the spin-1 deuteron is fully described by two structure functions involving three deuteron form factors [12–14]. The cross section is given by

$$\frac{d\sigma}{d\Omega} = \left.\frac{d\sigma}{d\Omega}\right|_{NS} \left[A(Q) + B(Q)\tan^2(\theta/2)\right] \equiv \left.\frac{d\sigma}{d\Omega}\right|_{NS} S_d(Q,\theta) \tag{1}$$

where

$$\left.\frac{d\sigma}{d\Omega}\right|_{NS} = \frac{\alpha^2 E' \cos^2(\theta/2)}{4E^3 \sin^4(\theta/2)} = \sigma_M \frac{E'}{E} = \sigma_M \left(1 + \frac{2E}{m_d}\sin^2\tfrac{\theta}{2}\right)^{-1} \tag{2}$$

is the cross section for scattering from a particle without internal structure (σ_M is the Mott cross section), and θ, E, E', and $d\Omega$ are the electron scattering angle, the incident and final electron energies, and the solid angle of the scattered electron, all in the lab system. The structure functions $A(Q)$ and $B(Q)$ depend on the three electromagnetic form factors as

$$\begin{aligned} A(Q) &= G_C^2(Q) + \frac{8}{9}\eta^2 G_Q^2(Q) + \frac{2}{3}\eta G_M^2(Q), \\ B(Q) &= \frac{4}{3}\eta(1+\eta)G_M^2(Q), \end{aligned} \tag{3}$$

TABLE I: Some measurements of A.

Experiment	Q (GeV)	Symbol	# of points	Year and Reference
Monterey	0.04 - 0.14	□	9	1973 [15]
Mainz	0.04 - 0.39	◯	16	1981 [9]
Saclay ALS	0.13 - 0.84	◊	43	1990 [10]
Orsay	0.34 - 0.48	△	4	1966 [16]
Stanford	0.48 - 0.88	□	5	1965 [17]
DESY	0.49 - 0.71	◊	10	1971 [18]
CEA	0.76 - 1.15	×	18	1969 [19]
JLab Hall C	0.81 - 1.34	⋆	6	1999 [4]
JLab Hall A	0.83 - 2.44	□	16	1999 [3]
SLAC E101	0.89 - 2.00	+	8	1975 [20]

with $\eta = Q^2/4m_d^2$. In many kinematics the contribution of $B(Q)$ to the cross section is small and $A(Q)$ can be reliably extracted from the cross section without a Rosenbluth separation. In the kinematics of this proposal, $B(Q)$ generally contributes $< 1\%$ to the cross section.

A selection of the world data set for $A(Q)$ is shown in Figure 2 and summarized in Table I. (The same symbols are not used in all of the figures.) More complete listings can be found in [5], or in the recent reviews [6–8]. We use a "fit" function to take out much of the momentum dependence of the data, so that differences not visible on a several decade semilog plot can be seen. The fit employs parameterizations of each of the three form factors that have the correct $Q = 0$ limit, and asymptotic fall offs as expected from a simple potential model. The "fit" structure functions are then generated from the "fit" form factors in the usual way, following Equation 3. We do not claim any theoretical significance for these "fit" functions; they are used simply to allow linear plots that emphasize differences.

Of particular interest to this proposal are the high precision lower Q measurements from Mainz [9], Saclay [10], and Monterey [15]. The main point from Figure 2 is that in the region of $Q \approx 0.2$ - 0.4 GeV, the Mainz (and lowest Q Orsay) data are about 10% larger than are the Saclay data, a very significant difference given the ≈1 - 2% claimed uncertainties of the experiments. The difference between the data sets is also of significance to the theoretical interpretation. We now review the theoretical calculations and demonstrate the importance of resolving the discrepancy. Afterward, we will return to the data and examine it in more detail; we shall show below that there is some internal evidence of small problems in both of the data sets.

Theoretical Calculations

Because a number of reviews have recently appeared covering deuteron elastic scattering [6–8], we will in this proposal focus on the results of the calculations at low Q; we will not discuss in detail the theoretical input and calculation procedures, which can be found in the reviews and in the original articles.

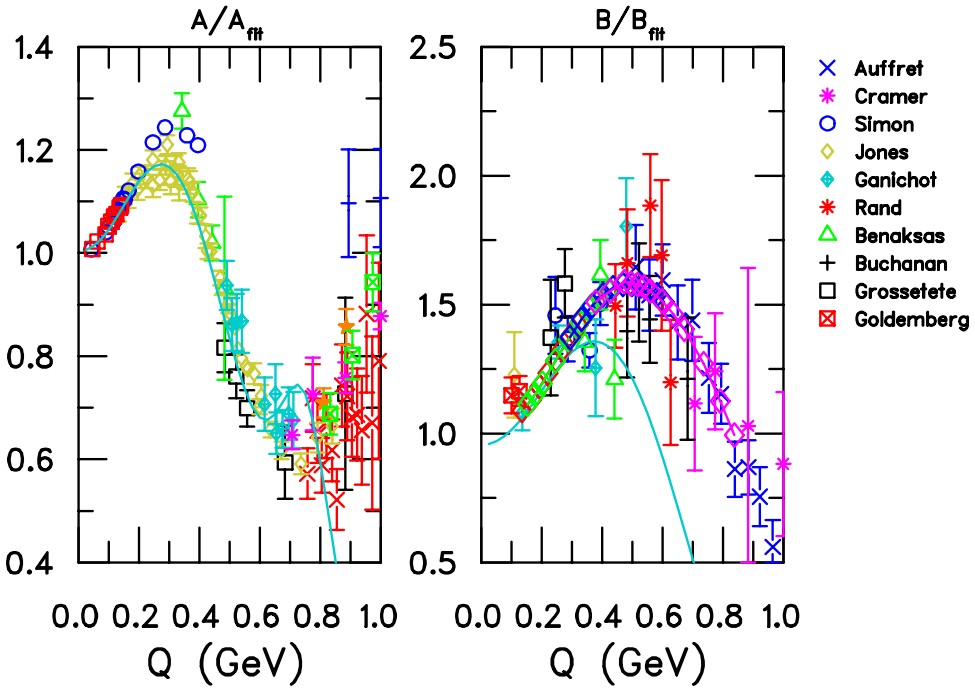

FIG. 3: χPT calculation of the deuteron A and B structure functions compared to data. The data and curves were divided by the corresponding A and B fit functions. The first authors of the B references are listed to the right of the figure, see [5–8] for the references.

Low momentum transfer calculations, related to QCD

Figure 2 showed pionless EFT ($\not\pi$EFT) calculations, from the recent work of Phillips, Rupak, and Savage [21] (PRS), applied to $A(Q)$. The NNLO calculation gives factor of two agreement with the data for momentum transfer up to $Q \approx 0.25$ GeV. While this $\not\pi$EFT is extremely useful for understanding the static properties of the deuteron and the structure for very low Q, it is limited in applicability to perhaps Q up to $2m_\pi$; it is unlikely that the measurements we propose here will be described by this theory.

Several χ perturbation theory (χPT) calculations have also appeared. Figure 3 compares the $A(Q)$ data to a recent calculation [22] using χPT wave functions for the deuteron, with the χPT current operator at NNLO. Once NN phase shifts have been fitted, the calculation to this order is essentially parameter free, with only a choice of the nucleon form factor parameterization - the *MMD* parameterization [23] was used - and a question about to what order the calculation must be carried out so that it has converged. Because χPT includes pions, the calculations are applicable up to much higher momentum transfers than is the $\not\pi$EFT calculation. Figure 3 shows that precise agreement[2] between χPT and the A data

[2] One has to worry about the possible logical circularity of the agreement of this and other theories. The MMD fit uses the Saclay extraction of G_{En} from their A data. Insofar as the wave function model and corrections are similar, other calculations should then reproduce the Saclay data. The relativistic VOG calculation in contrast uses the MMD form factors but agrees better with the Mainz data. This situation

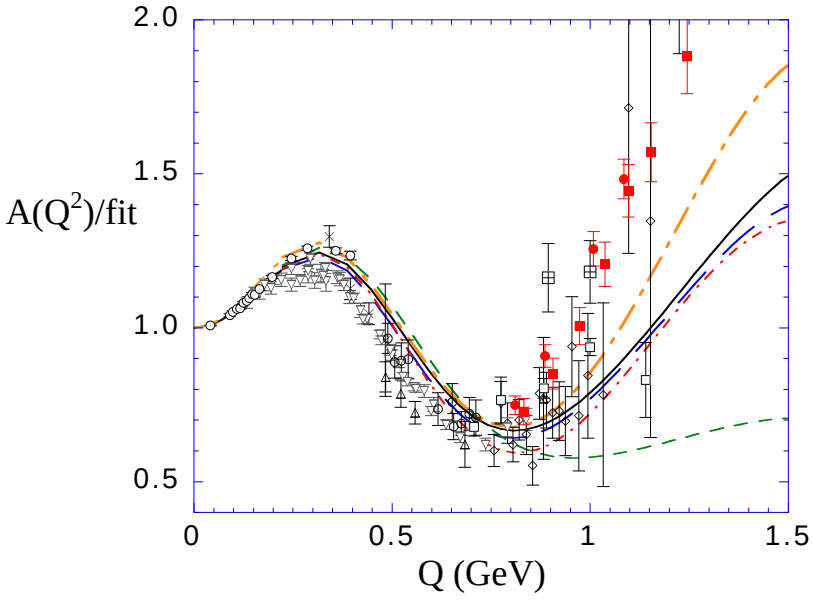

FIG. 4: The data for A at low and moderate Q, divided by the fit function, compared to five nonrelativistic calculations described in the text.

- assuming the Saclay data are correct - is possible up to momentum transfers of perhaps 0.6 GeV. With the B data, which has only 20% or so uncertainties, the agreement is only good up to 0.3 GeV; it is expected that there is a larger short distance contribution to B and thus the convergence of the theory for B is not as good. If the Mainz A data are more nearly correct, it would be necessary to continue the calculation to higher order, which will include terms that have to be determined from the form factor data. Presumably the next order would then improve agreement with both A and B. If the Saclay A data are more nearly correct, higher order corrections are significant for B but nearly vanish for A. These recent results represent an improvement on the earlier work of [24]. The recent calculation of [25], which also claims technical improvements upon [24], tends to overpredict G_C and G_M, while underpredicting G_Q.

Conventional nonrelativistic calculations

A set of conventional nonrelativistic calculations, with *no meson exchange currents* or other corrections, is shown in Fig. 4. In this limit, the deuteron properties depend solely on the wave functions. The calculations (in order of decreasing magnitude at $Q = 0.1$ GeV^2) use W16 (long dot-dashed), CD Bonn (short dashed), AV18 (solid), IIB (short dot-dashed), and Paris (long dashed) wave functions. The W16 and IIB models use the S and D wave functions of a relativistic model, neglecting the P-state components. The variation of these

is gradually becoming resolved with increasing amounts of polarization data as input to nucleon form factor fits.

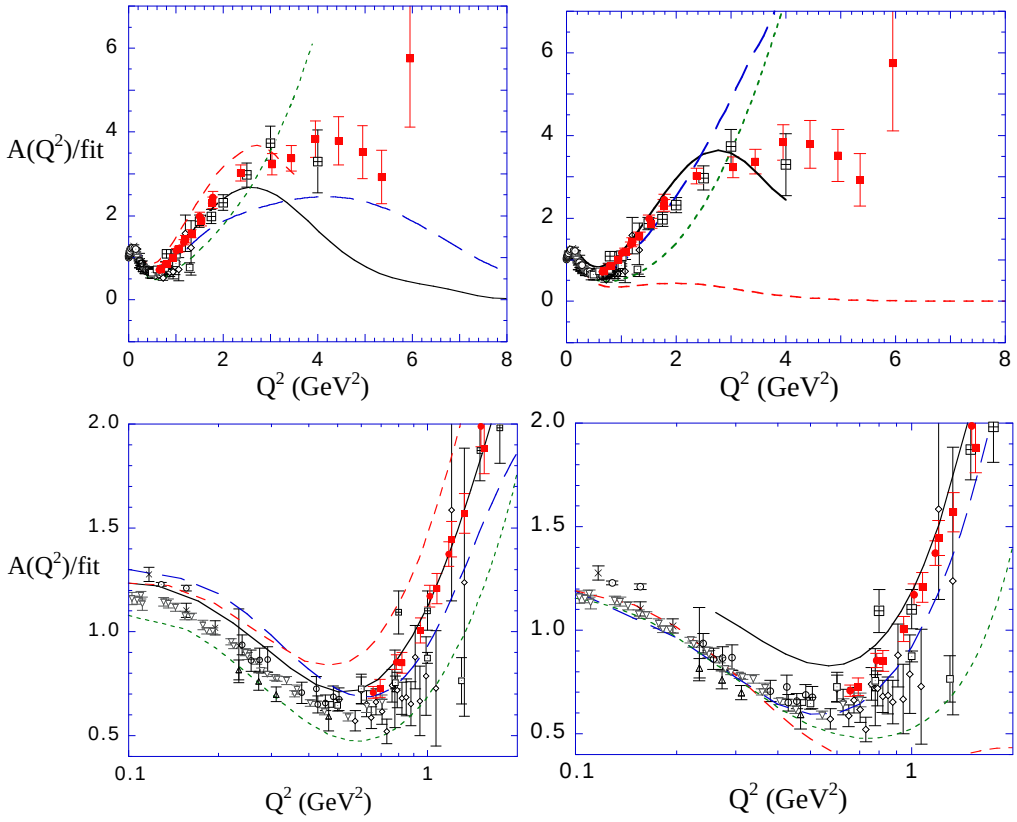

FIG. 5: The data for $A(Q)$, compared to eight relativistic calculations. Left panels show the propagator and instant-form results: FSR (solid line), VOG in RIA approximation (long dashed line), ARW (medium dashed line), and PWM (short dashed line). Right panels show the front-form CK (long dashed line) and LPS (short dashed line), the point-form AKP (medium dashed line) and the quark model calculation DB (solid line).

models is only about $\pm 2\%$, and the models are generally higher (lower) than the Saclay (Mainz) data. Since the two data sets tend to fall on opposite sides of the nonrelativistic calculations, it becomes unclear whether the leading order relativistic corrections are positive or negative.

The close agreement of these nonrelativistic calculations is not very surprising, as all are based on modern, low χ^2 fits to the NN phase shifts. The lack of sensitivity to the details of these models is an important point. It indicates that in the low Q region where the differences between the data and the calculations far exceeds the differences among the calculations, the sign and approximate magnitude of relativistic corrections can be reliably extracted. For these wave function only models, adjusting the potential is the only freedom available, but it will worsen agreement with NN scattering. It is clear other physics is important. In the conventional framework, the corrections may all be viewed as being of relativistic origin, and we now turn to relativistic models.

Relativistic and quark model calculations

Figure 5 compares seven relativistic calculations and one quark model calculation to the $A(Q)$ data. All of these calculations were done without the "famous" $\rho\pi\gamma$ meson-exchange current, which is not well understood, and has a negligible effect in the Q regime of this proposal. The calculations include both covariant/field theory formulations and Hamiltonian dynamics (instant, point, and front form) calculations. The calculations, ordered from largest to smallest at $Q^2 = 0.1$ GeV^2 are:

Van Orden, Devine, and Gross (VOG) [26]: propagator formulation using the relativistic impulse approximation and the Gross equation (left panels, long dashed line)

Forest, Schiavilla and Riska (FSR) [27]: Hamiltonian instant form with no v/c expansion (left panels, solid line)

Arenhövel, Ritz and Wilbois (ARW) [28]: Hamiltonian instant form with a v/c expansion (left panels, short dashed line)

Allen, Klink, and Polyzou (AKP) [29]: Hamiltonian point form (right panels, medium dashed line)

Carbonell and Karmanov (CK) [30]: Hamiltonian front-form with a dynamical light front (right panels, long dashed line)

Lev, Pace, and Salmé (LPS) [31]: Hamiltonian front-form with a fixed light front (right panels, short dashed line)

Phillips, Wallace, Devine, and Mandelzweig (PWM) [32]: propagator "equal-time" formulation using the Mandelzweig and Wallace equation (left panels, dotted line)

The solid line in the right panels is a nonrelativistic quark compound bag model calculation (DB). While there have been many investigations concerning the implications of pQCD and helicity conservation on the deuteron properties, these limits are clearly not of concern in the momentum range of this proposal.

An examination of Figures 4 and 5 shows that the nonrelativistic calculations tend to be about equal to or smaller than the ARW calculation, but definitely bigger than the CK calculation. The calculations of VOG, FSR, and ARW, which tend to agree better with the Mainz data, are more technically complete than are the calculations of AKP, CK, LPS, and PWM [8] which tend to agree better with the Saclay data. Thus, theoretical bias would suggest the correct trend is the Mainz, rather than the Saclay data. However, the larger amount of Saclay data, as well as the overlap with higher Q experiments from other labs, suggests instead that the correct trend is below the nonrelativistic calculations. It appears then that the relativistic corrections (that is, the net effect of including all physics beyond the nonrelativistic wave function only model) could be either positive or negative, are as much as several percent for the momentum transfers of this proposal, and may not be under control.

Figure 6 explores this issue an another context, using values for the charge form factor extracted from the $A(Q)$ measurements, using small corrections for the quadrupole and magnetic contributions, based on the simultaneous fits to A, B, and t_{20} [5]. There are several percent differences between the calculations, and these data are not sufficiently accurate to

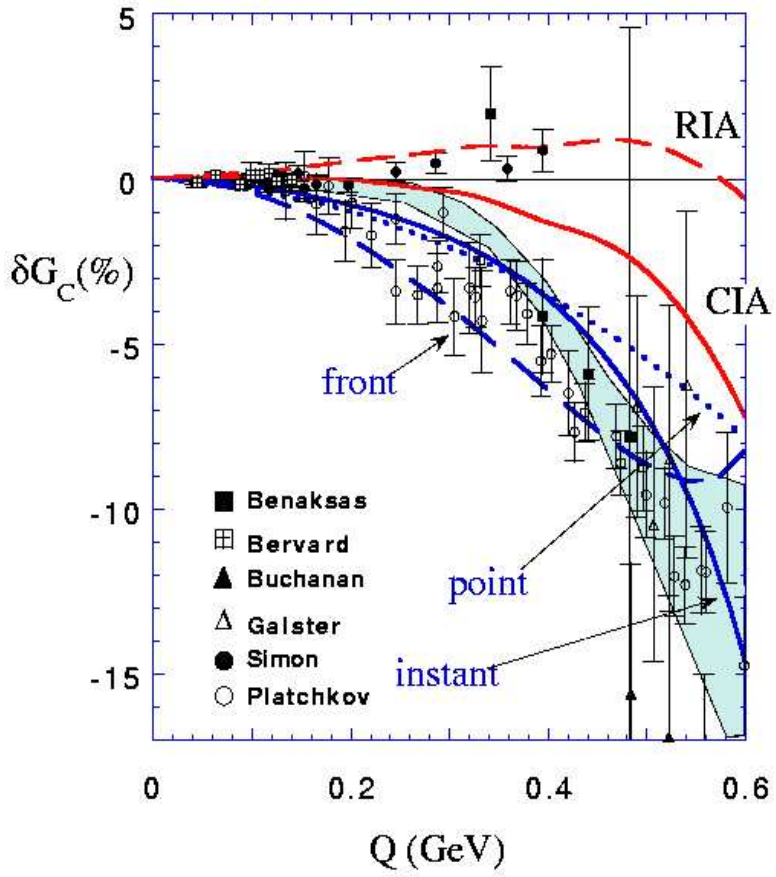

FIG. 6: Experimental data for G_C compared to five relativistic calculations, relativistic impulse approximation (RIA) and full calculation (CIA) from VOG, and point, instant, and front forms from AKP, ARW, and LPS, respectively. The shaded band indicates the typical range of fits to G_C. All data and curves are shown relative to the nonrelativistic AV18 potential calculation.

distinguish between the calculations. However, A is dominated by G_C at least up to ≈0.45 GeV, and these data are biased by the numerous Saclay data points to favor lower values of G_C; using only the Mainz data in his region would lead to a 3 - 4% increase in G_C, which would favor the RIA / CIA calculations.

Summary: comparison of theory to data

We have shown above that ∕πEFT can at present only describe the deuteron well at very low momentum transfers, perhaps up to Q of 0.1 - 0.2 GeV. χPT theory has been shown to give approximate agreement up to several hundred MeV in [24] and [25], and good quantitative agreement in [22] - if the Saclay $A(Q)$ data are correct. If the Mainz data are more correct, it will be necessary to perform a higher order calculation. $B(Q)$ is more poorly reproduced.

The nonrelativistic potential calculations lie between the Saclay and Mainz data sets, and have variations of 1 - 2%. This small variation makes it clear that a precision measurement

can determine the sign of the leading low-Q relativistic corrections. If the Saclay $A(Q)$ data at low Q are more nearly correct, the AKP, CK, and LPS calculations are in very good agreement with the data. If however the Mainz data are more nearly correct, the FSR and VOG calculations appear to be most accurate. If one examines the $B(Q)$ structure function - see Figure 1 - in particular in the region near the minimum, $Q \approx 2$ GeV^2, the VOG, LPS, DB, and FSR calculations are closest to the data. If one examines instead t_{20} - see Figure 1 - the LPS calculation is by far the least satisfactory. One might argue AKP and DB are also somewhat too negative after the minimum, but the other calculations are all more or less reasonable.

Thus, if the Mainz data are correct, both the VOG and FSR calculations provide a reasonable good account of the full data set. However, if the Saclay data are correct, it appears that *no* conventional calculation is entirely satisfactory.

As indicated above, our theoretical bias is that the VOG and FSR calculations are more complete and mature than the others. Thus it will be more difficult to improve these calculations if they are found to be in disagreement with the data. Perhaps the main point to take from this discussion is that there is a strong effort by many different theoretical groups to understand the deuteron structure. High precision data in the region of the discrepancy between the existing Mainz and Saclay data sets would be of great interest.

Extraction of G_{En}

One of the major aims, and highlights, of the Saclay experiment was the extraction of G_{En} from the elastic scattering data. Note that the $A(Q)$ in the Q range of this proposal is determined almost solely by the deuteron charge form factor, to within a few percent. In a nonrelativistic, purely wave function model for the deuteron, the deuteron elastic form factors arise from a product of deuteron body form factors multiplied by isoscalar nucleon form factors, e.g., $G_{Ep} + G_{En}$. (The expressions can be found in any of the recent reviews as well as a number of articles.) Thus, knowledge of the deuteron charge form factor and the proton electric form factors allows a direct calculation of G_{En}. In the range of the Mainz data G_{Ep} is close to unity, and well known, while G_{En} is perhaps 0.05. With $A \propto G_C^2$, 5 - 10% changes in A lead to 0.025 or 0.05 changes to G_{En}. Of course, this simple analysis is not entirely correct as it neglects the relativistic corrections, which, based on the calculations and data, are small in the lower Q region of this experiment, but of similar size to the contribution of G_{En}.

Recent polarization experiments have provided several data points, with much reduced sensitivity to the reaction mechanism, which generally imply that G_{En} is slightly larger than in the Saclay analysis, 0.05 - 0.06 rather than the 0.04 of the Saclay analysis. The variations of the theories indicate potential difficulties with the relativistic corrections for the extration of G_{En} from measurements of $A(Q)$ with good precision. From a different perspective, the larger values of G_{En} suggested by the polarization measurements would tend to make all the calculations of G_C or A larger, making the VOG and FSR calculations more in favor the Mainz data, and raising the other calculations to be even with or above the Saclay data. Since the polarization experiments are so difficult, it is desirable to extract G_{En} from the cross section measurements. A new high-precision data set might give confidence that such an extraction can be made with one of the more modern complete theories.

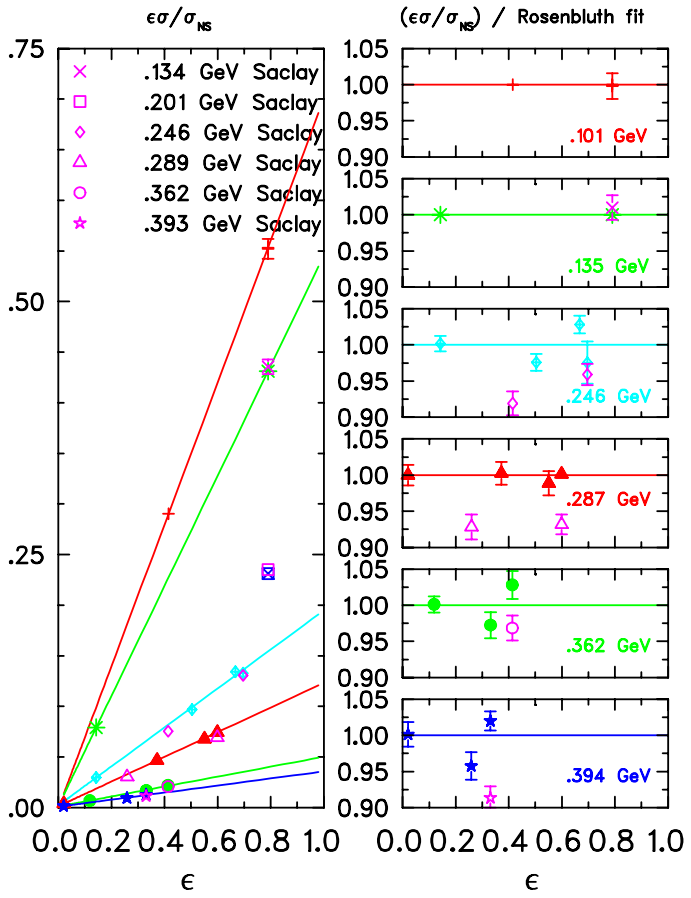

FIG. 7: The left panel shows Rosenbluth separations for the Mainz data. Saclay data at essentially the same Q are given by the corresponding open symbols. (The 0.20 GeV data are shown as an additional check of the overlap of Saclay and Mainz cross sections; there are insufficient data for a separation.) The right panel shows the data in detail using the ratio of the data points to the Rosenbluth separation, so that the consistency of the points can better be seen. Some of the variation arises from the points being at slightly different Q values.

Evaluation of low Q experiments

In this section, we describe in greater detail the three high precision data sets for the deuteron A structure function at low Q.

The Monterey experiment [15] (red open squares in Figure 2) measured a ratio of elastic *ed* to *ep* scattering using cooled gas targets and electron energies up to 105 MeV. Thirty-three ratios were used to determine the deuteron $A(Q)$ structure function, and thus G_C, for nine different Q points - for these very low Q points, G_C accounts for ≈99% of the cross section. The claimed relative systematic uncertainty of the deuteron to hydrogen cross section ratio was ≈0.3%.

The Mainz experiment [9] (blue open circles in Figure 2) used liquid and gas targets to determine elastic cross sections at 8 beam energies, from 80 to 298.9 MeV, with laboratory electron angles from 30° to 157°. The claimed deuteron cross section systematic uncertainty

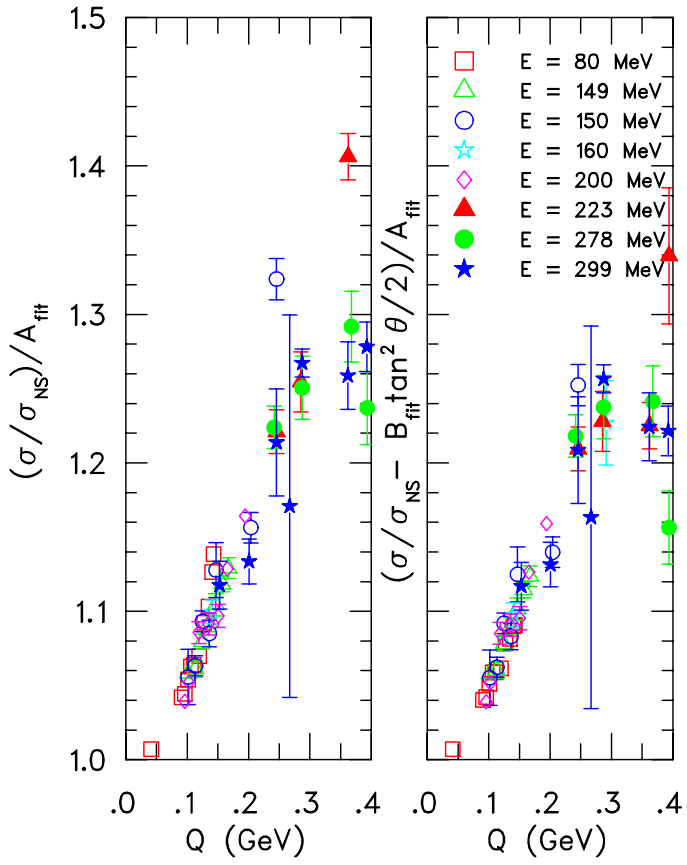

FIG. 8: The Mainz reduced cross sections, at low Q. The data in the left panel are divided by the fit function for $A(Q)$, which, by not including an angle correction, should leave lower energy data systematically higher than the higher energy data. The data in the right panel have an estimate of the $B(Q)\tan^2(\theta/2)$ contribution subtracted before being divided by the $A(Q)$ fit function. The subtraction should roughly bring all data sets into alignment.

was ≈0.7%, with the normalization checked with hydrogen data. For the smaller Q Mainz data, $B(Q)$ is too small to be measured, and corrections were calculated. For the four highest Q points, the points for which there is the disagreement with the Saclay data, $B(Q)$ was determined by a Rosenbluth separation.

Figure 7 shows $\frac{d\sigma}{d\Omega}/\epsilon\frac{d\sigma}{d\Omega}|_{NS} = \Big[A(Q)+B(Q)\tan^2(\theta/2)\Big]/\epsilon$ as a function of ϵ for these data[3], as well as for some of the Saclay data. The Rosenbluth fits are also shown[4]. It is apparent that at most of the Q values the spread in the forward angle, high ϵ, points is larger than desirable. Most of the spread is related to the points not being exactly at the same Q. The most forward angle, high energy, large ϵ points were taken at 298.9 MeV beam energy, and scattering angles of 50°, 60°, 80°, and 90°. The contribution of $B(Q)$ to the cross section

[3] The Mainz publication [9] only did separations for the four higher Q values shown; uncertainties on B were too large to be meaningful at the lower Q values.

[4] The fits are not constrained to be 0 at $\epsilon = 0$; B is small.

ranges from about 0.5% to 5% for the forward angle points at each of these Q.

We further examine the self-consistency of the Mainz data by comparing reduced cross sections in Figure 8. Here it can be seen that there are more or less normal statistical fluctuations in the data, and that an approximate correction for the B contribution brings the data into better alignment; two of the backward angle higher Q points that are off scale in the left panel come into reasonable agreement in the right panel. [5]

The Saclay data [10] (brown open diamonds in Figure 2) used 4 energies from 200 to 650 MeV, with scattering angles from 35° to 100°. Careful attention was paid to systematic effects including detection efficiencies and solid angles. The contribution of $B(Q)$ to the cross section was calculated, based on previous measurements, and subtracted. The claimed systematic uncertainties were 1 - 1.5%. The disagreement with the Mainz measurements comes most directly from four 300 MeV data points, for which the reduced cross sections ($\frac{d\sigma}{d\Omega}/\frac{d\sigma}{d\Omega}|_{NS}$) disagree with those of the 298.9 MeV Mainz data *at the same scattering angles* by about 10% - see Figure 7. (The difference in Q and σ_{NS} for the 1 MeV change in energy leads to only a ≈1% correction.) It can be seen in Figure 7 that the Saclay data are slightly lower than the corresponding Mainz data, and further, for $Q = 0.248$ GeV, the Saclay data even indicate $B(Q) \approx 0$, since it is required to be nonnegative. The Saclay article mentions, without explaining, the disagreement with Mainz.

We examine the Saclay reduced cross sections more closely in Figure 9. In the left panel we have divided by the fit function for $A(Q)$ only, to remove much of momentum dependence *without* introducing any angle dependence related to the $B(Q)$ correction. In the right panel, an approximate correction is made for the $B(Q)$ contribution. The main point is that the lower beam energy data should be equal to, or slightly above, the higher beam energy data, due to the larger contribution from $B(Q)$ at the larger scattering angle, but the lower Q Saclay data are *inconsistent* with this principle. The 200 MeV data (stars) are *systematically less* than the 300 MeV data (circles), and the 300 MeV data (circles) are *less* than the first few 500 MeV data points (triangles). [6] For points below $Q = 0.3$ GeV, the 200 MeV data are systematically 2% below the 300 MeV data. Thus, it is reasonable to question whether there is a normalization problem in the Saclay data, particularly for the low energy data sets, which might affect theoretical interpretation. However, the level of the disagreement is within the quoted systematic uncertainties of the measurement.

To summarize, while the overlap of the lower Q Mainz data looks good, the higher Q data for which the Rosenbluth separations were performed shows more variation than is desirable. The overlap of the Platchov data from different energies indicates systematic deviations can be seen up to $Q \approx 0.35$ GeV. Thus, it appears that the underlying source of the variations in the low Q Saclay $A(Q)$ values shown in Figure 2 is a systematic energy to energy variation, rather than a random point to point variation. Given the overall uncertainties, probably neither of these problems would be taken by themselves to indicate definite problems in the

[5] In the published Mainz data table, there are four kinematic points for which the quoted cross section is inconsistent with the quoted reduced cross section. For three of the points the difference is exactly a factor of 10, while for the fourth point the difference is a factor of 12.5. In each case, we have used the published reduced cross section value. The large, ≈10% uncertainty, on the $Q = 0.27$ GeV point is as published.

[6] Note that for a high precision comparison, it is also necessary to study Coulomb corrections, as was done by Sick and Trautmann[33]. This correction appears to be a few tenths of one percent, in the overlap of the Saclay data at the different energies.

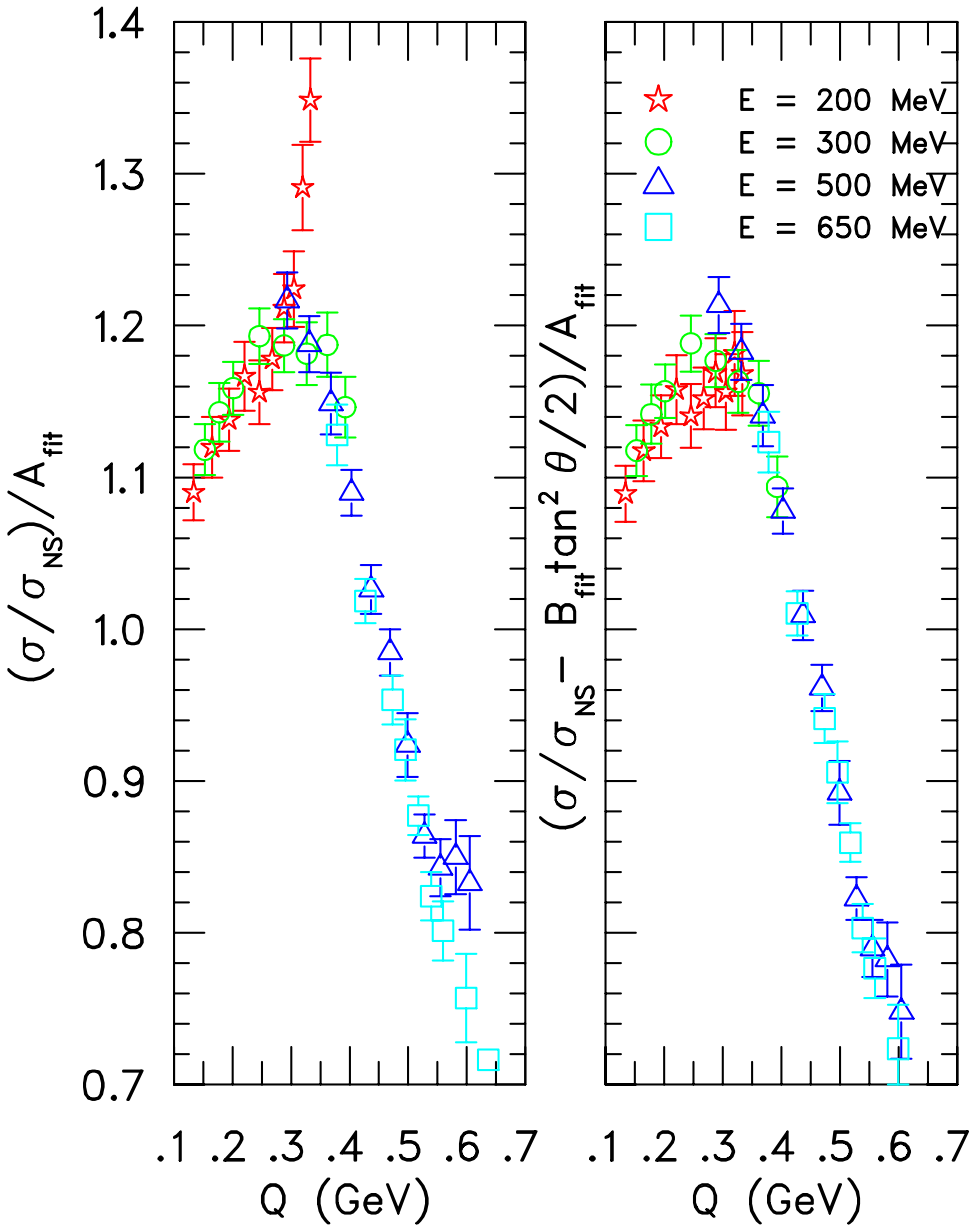

FIG. 9: The Saclay reduced cross sections, at low Q. The data in the left panel are divided by the fit function for $A(Q)$, which should leave lower energy data systematically higher than the higher energy data. The data in the right panel should be roughly aligned.

data. It is only in the context of the disagreement of the two experiments, and the desire for a very precise result to distinguish theories, that if becomes clear that a new high precision measurement should be performed to resolve the discrepancy between the two data sets.

PROPOSED MEASUREMENTS

The goal of this experiment is to attempt to put the comparison of theory to experiment on a firmer basis, by measuring precise and accurate cross sections that will both distinguish between the Mainz and Saclay data sets, and improve upon them. We will do this primarily by determining the absolute *ed* elastic cross section to <<1 % statistically and to 2 - 3 % systematically over much of the region of $0.2 < Q < 0.8$ GeV/c. To ensure that these data are sufficient and well calibrated, we will also determine even more precisely cross section ratios for each point, as well as the Q dependence of the *ed* cross sections, which allows determination of a precise $A_{relative}(Q)$. We will make each measurement with both Hall A spectrometers to provide an additional cross check. As a final cross check, we will repeat the measurements at a second beam energy. Because these measurements are performed at "high energy", relative to previous experiments, the contributions of $B(Q)$ are small, $\leq$1 % for all but our highest momentum transfer settings. The important experimental issue is keeping systematic uncertainties under control. Aspects of this include knowing the scattering angle and integrated beam current, keeping count rates from being too large, and being able to prove that the data are self consistent and accurate. Having a measurement at a second energy, for which $d\sigma/d\Omega|_{NS}$ is different, is an important step in demonstrating that we have correctly evaluated the systematic uncertainties.

Absolute cross section measurements

The cross section is directly determined from the measured counts through

$$\frac{d\sigma}{d\Omega} = \frac{Counts}{L_t} \cdot \rho_t \cdot \frac{Q_b}{e} \cdot \Delta\Omega \cdot R \cdot \Pi_i \epsilon_i \tag{4}$$

Where L_t is the target length and density, ρ_t is the target density in atoms/cm^3, Q_b is the beam charge and e is the electron charge, R is the radiative correction factor, and $\Pi_i \epsilon_i$ is the product of efficiency correction factors, which includes the efficiencies of and dead time corrections for the detectors, the trigger, the DAQ, and track reconstruction. Experiments that have paid careful attention to systematics in Hall A have been able to determine absolute cross sections to about 2 %, in particular during optics studies using elastic scattering at moderate currents on a thin ^{12}C target of precisely known thickness. In addition to the uncertainties on these factors, one must know how backgrounds affect the yield and the Q value at which the data are taken.

The most recent high precision cross section measurement in Hall A was E01-001; these *ep* elastic scattering "super-Rosenbluth" data were taken in mid 2002. The experiment used a 70 μA beam current and a 4 cm LH_2 target to measure Rosenbluth separations, detecting the proton at constant momentum transfer for a series of beam energies. The claimed systematic uncertainty[34] is 3 % (0.45 %) for the absolute (point-to-point) cross sections. The contributions to the uncertainty are shown in Table II.

Besides the demonstration of the ability of Hall A to measure precise cross sections, E01-001 had two other important results from the perspective of this update. First is a confirmation of earlier studies of the knowledge of the spectrometer central angle. This calibration now appears to be good to 0.3 mr, rather than the 0.6 mr typically quoted

earlier.[7] Second is a thorough study of spectrometer backgrounds that indicated how the backgrounds can be precisely subtracted.

As compared to the results of E01-001, we have various factors that make our measurements both easier and harder. Measuring over a shorter time scale at constant beam energy reduces uncertainties for us, but measuring at constant momentum and with nearly constant count rates reduces uncertainties for E01-001.

TABLE II: Dominant cross section uncertainties from Hall A E01-001. The relative uncertainty from the luminosity is negligible, except for the 2.26 GeV data taken at a lower beam current, 30 - 50 μA.

Item	$\Delta\sigma_{abs}$ (%)	$\Delta\sigma_{rel}$ (%)
Solid angle	2	-
Radiative correction	1	0.2
Background subtraction	1	0.2
Luminosity	1	0 - 0.3
Tracking efficiency	-	0.2
Scattering Angle	-	0.2
Total	3	0.45

Detectors and backgrounds

The scattered electrons will be detected in the HRS spectrometers with their standard detector packages, which consist of trigger scintillators, VDC chambers, gas Cerenkov detectors and double-layer shower counters. Elastic scattering measurements are relatively clean, due to the lack of higher energy particles scattering from the magnet pole faces. At the low energies of the experiment, and in elastic kinematics, the π^- background is minimal and easily removed with PID cuts. A coincidence of scintillators S1 and S2 provides the standard trigger, and efficiencies are checked with a trigger that has a reduced scintillator hit requirement, but also requires the gas Cerenkov or an additional trigger scintillator, S0, to fire.

In addition to the deuteron events, there will be events coming from the target cell walls; these will be subtracted by an empty target measurement. The experimental resolution is limited primarily by multiple scattering and the determination of scattering angle, but it is sufficient to cleanly separate the *ed* elastic peak from threshold electrodisintegration in all kinematics. Also, the threshold disintegration is suppressed at the forward angles of

[7] An even better result has been achieved, through the use of *ep* elastic scattering and beam energy measurements. Ibrahim, Ulmer, and Liyanage [35] demonstrated that the HRS angles could be determined to 0.1 - 0.2 mr. We do not plan to adopt this technique here as the precision is most important for the low Q points, leading to a very low energy backward proton.

TABLE III: Estimated cross section change (in percent) for changes in kinematic parameters, for $E = 0.857$ GeV and the Q points we propose to measure. Also shown is the estimated contribution from the $B(Q)$ structure function to the cross section in %. For the same Q points, the cross section changes increase with beam energy, while the $B(Q)$ contribution decreases with beam energy. The size of the systematic changes given are the 1σ estimates for these parameters in Hall A.

Q (GeV)	δ_E of 0.02 %	$\delta_{E'}$ of 0.04 %	δ_θ of 0.3 mr	Total	$B(Q)$
0.20	0.08	0.00	0.78	0.78	0.02
0.25	0.09	0.02	0.69	0.74	0.04
0.30	0.09	0.03	0.62	0.63	0.08
0.35	0.10	0.04	0.56	0.57	0.15
0.40	0.10	0.05	0.52	0.53	0.25
0.45	0.11	0.06	0.48	0.50	0.40
0.50	0.11	0.06	0.44	0.46	0.60
0.60	0.12	0.08	0.39	0.42	1.22
0.70	0.13	0.09	0.34	0.37	2.21
0.80	0.13	0.11	0.30	0.34	3.81

this measurement; existing threshold disintegration data were obtained in more favorable large-scattering-angle kinematics.

As compared to E01-001, backgrounds in this experiment are less of a problem. The main background in E01-001 to measuring singles protons in ep elastic scattering is protons from the process $\gamma p \to p\pi^0$, for which the end point is close to or overlapping the ep elastic peak, particularly at high energies. There is no comparable pion production process in measuring elastically scattered electrons at low beam energies.

Determination of Q

Since $A(Q)$ is a steep function of Q, it is important to know the kinematics of the measurements well. Table III shows the sensitivity of the cross sections to the beam and scattered electron energies, and to the scattering angle. For this calculation, these quantities were treated as all independent, even though only two of the three are.

The beam energy will be determined by ARC and EP measurements; once these absolute energy measurements have been done, the stability of the beam energy can be reliably monitored from magnet settings and beam position monitors. The recent hypernuclear experiment in Hall A found that the beam energy was stable to a few parts in 10^5, and the beam energy spread was of similar size, despite running in parallel with the G0 experiment in Hall C. The spectrometer constant is known well enough to determine the outgoing energy to 0.04 %. The determination of Q with these quantities also requires correcting for energy loss in the target.

The largest systematic is related to the determination of the absolute scattering angle. Two sets of beam position monitors upstream of the scattering chamber will provide infor-

mation on beam incident angle (to 0.1 mr) and beam position. The spectrometer pointing is determined by multiple systems. The pointing, as well as the solid angle and y_{target} calibration, will be checked with ^{12}C,^{181}Ta(e,e') data at each angle. The absolute angle and spectrometer constant are checked at each angle through elastic scattering on multiple targets, including ^{1}H, ^{2}H, ^{12}C, ^{27}Al, and ^{181}Ta[8]. The uncertainty of 0.3 mr on the absolute scattering angle comes from the uncertainty in the position of the sieve slit relative to the spectrometer, which ends up dominating the uncertainty in Q. This number is a factor of two better than believed at the time we submitted the original proposal.

Beam charge - the "silver" calorimeter

Knowing the integrated charge for absolute measurements is one of the most difficult issues. (Of course, only the relative charge is needed for angle dependences and for the deuterium to hydrogen ratios.) The general system in Hall A is to determine the charge in the Hall with precise relative beam current monitors (BCMs) which are calibrated to an Unser monitor. Operational experience in Hall A is that current calibrations, are good for higher currents to $\approx$1 %, and, once performed, are stable at the 1 % level for months. The two BCMs are each read out with three V to F converters; the variation of these plus the Unser monitor, allows cross checks at the $<<$1 % level. The systems have not been as extensively studied for currents below about 3 μA; as we are operating at lower currents for part of the experiment, we will need to carefully perform calibrations. We will require several hours of facility development time to calibrate and study the calibration, and its time variation, at low currents.

Since E02-004 was approved, we have been working on the design of a "silver" calorimeter[9] to enable Hall A to calibrate the beam current for low currents, from a few hundred nA to a few μA. The calorimeter is based on a SLAC device which was operated with about 1 % precision, but several design improvements have been incorporated. The calorimeter is a total absorption device; it measures the total energy deposited in the calorimeter slug through the temperature change of the slug. The heat capacity of the slug is calibrated using a precision power supply to deposit a well known (and measured) heat load into the slug. The integrated beam current is then determined from the measured beam energy. The calorimeter is used at regular intervals to provide an absolute calibration for the BCMs, which are then used for the experimental data.

A design review was performed for the project in mid 2004. An overview of the mechanical design of the system is shown in Fig. 10. The calorimeter team includes Michael Bevins, Tony Day, Pavel Degtyarenko, and Arne Freyberger of Accelerator Division, along with Eugene Chudakov, Ron Gilman, and Arun Saha from Physics Division. Studies of the electronics associated with the project indicate that 10^{-3} precisions are achievable. Thermometry is good to about 20 mK, out of a typical 30 K temperature rise, without even including averaging over time to improve precisions. We conservatively estimate the knowledge of the temperature rise will be 0.2 %, and this knowledge will also limit the calibration of

[8] As we go to higher Q points, data rates fall for the heavier targets, but they are less needed and will be eliminated.

[9] We ultimately chose to use a tungsten copper alloy for the calorimeter slug instead of silver, as it provides significant reduction in hadronic and EM shower losses, and their associated uncertainties.

TABLE IV: Estimated uncertainties for the beam calorimeter determination of the absolute Hall A beam current.

item	loss (%)	uncertainty (%)
beam energy	-	0.02
ΔT	-	0.20
heat capacity	-	0.20
heat losses	0.40	0.10
EM showers	0.15	0.05
hadronic losses	0.30	0.15
TOTAL	0.85	0.34

the slug heat capacity. Energy is also lost through radiative and conductive heat losses over the several minute time of the measurement, and through EM showers and hadronic interactions in the slug resulting in particles that are not contained in its volume. An example of a hadronic loss is low-energy neutrons from the decay of photo-excited giant resonances escaping the slug. These hadronic and EM shower losses are energy dependent, but are estimated to be typically a few tenths of a percent. For this proposal, we conservatively estimate the current will be known to 0.5 % absolutely and to 0.1 % relatively. The estimated losses and uncertainties for the calorimeter that were presented at a design review at Jefferson Lab are summarized in Table IV.

The design of the calorimeter is now essentially complete, and procurement has started on various parts of the device. Important parts of the electronics system have been purchased, and are being tested on an aluminum slug to verify performance. It is expected that the calorimeter construction will be completed in time to allow installation during late 2005 [36]. This will allow development time for the calorimeter so that its performance can be thoroughly studied before the experiment is scheduled, hopefully late 2006 or early 2007.

Cryotarget

The standard 4 cm Hall A cryotarget cells are sufficient for this proposal. For these cells, the cryotarget length and density can each be determined to $\approx$0.15 %, leading to a 0.2 % uncertainty in its areal density. Density variation from target boiling is not an issue at low currents; also we will use one spectrometer as a fixed monitor while varying the angle of the second spectrometer, so that relative luminosity will be measured precisely, to $\approx$0.1 %. Furthermore, for ratios of deuterium to hydrogen cross sections, the relative density between the H and D targets is known to 0.3 %.

As indicated above, we plan to use targets of ^{1}H, ^{2}H, ^{12}C, ^{27}Al, and ^{181}Ta. The standard Hall A target configuration has space for up to three cryogenic loops, each with long and short cells (^{1}H, ^{2}H, and spare), an optics target (multiple thin carbon foils), dummy targets for the cryogenic cells (^{27}Al), three solid targets (^{12}C, ^{181}Ta, and BeO), and an empty target position. The optics targets are used in optics calibration runs, while the solid targets are used in spectrometer pointing runs, plus for the angle calibration. Since the experiment

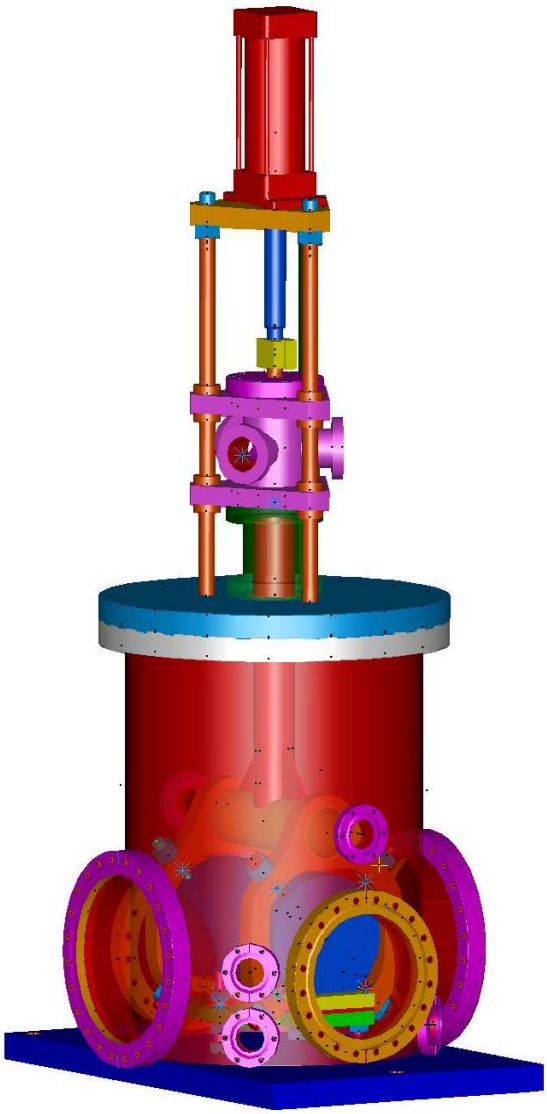

FIG. 10: Three-dimensional CAD view of the beam calorimeter system mechanical design. The large vacuum cylinder has a ≈40 cm in diameter, and is rendered semi-transparent so the calorimeter can be seen inside.

will be running with very low currents (except for Kin-8_d, Kin-9_d, and Kin-10_d), cryotarget density fluctuations caused by beam heating are negligible. The target density will be determined through temperature and pressure measurements.

Solid angle

Calibrations in Hall A with a thin ^{12}C target have determined the HRS solid angle to ≈1 %, and absolute cross sections to 2 - 3 %. For this proposal, with a 4-cm cell, we will be operating with a *slightly* extended target, with $\Delta y_{target} = \pm$ 0.5 – 1.8 cm. The absolute

solid angle will be determined by using the multiple carbon foil target, to nearly 1 %. The solid angle for the ratio measurements of D to H is essentially identical, since we measure at the same spectrometer angle with the same extended target.

Radiative corrections

Radiative corrections for the hydrogen and deuterium are very similar, and cancel in the relative cross sections, but for the absolute cross sections they are about 40 %, varying by ± 5 % across our angle range. The uncertainty in R will be about 1 % absolute, and much smaller in the relative measurements.

Efficiencies

Care must be taken with the forward angle data, for which the raw count rate will be $\approx$100 kHz. By taking prescaled data with two independent, but commonly gated, data acquisition systems, as was done for the g_2^n experiment, E97-108, during summer 2001, it will be possible to have small DAQ dead times which can be precisely corrected. Scintillator and trigger dead times are also small. Scintillator efficiencies are monitored by having a tight trigger, which requires all four phototubes on scintillator paddles in S1 and S2 to fire, as well as a loose trigger that is used to study the inefficiency. Having the two independent DAQs limits the number of trigger types and the uncertainty in the dead time corrections. The largest difficulty is multiple tracks in the VDCs, which lead to an uncertainty in the tracking efficiency at high rates. The VDCs have a maximum drift time of about 0.25 μs. At 100 kHz rate, there is a $0.25\mu\text{s}/10\mu\text{s} = 2.5$ % probability of a second event leading to signals seen in the drift chamber. Most of these events will not cause problems as they will be spatially separated from the triggering event, and, depending on the relative timing, either the long or short drift times will be eliminated from the event analysis. The exact level of the uncertainty depends on the quality of the tracking algorithms, and the ability to recognize and remove poorly tracked events from the data without biasing it - one has to distinguish between events that really should not have a track and events for which the tracking did not produce a good track.

Hydrogen ratio measurements

As indicated above, the deuteron elastic form factor $A(Q)$ will be extracted directly from the cross sections to better than $\pm 3\%$ accuracy. Because proton and ^{12}C elastic scattering are well known, we will also determine these cross sections at each point, to check our experimental procedures and to allow the deuteron $A(Q)$ form factor to be extracted relative to these cross sections, from the ratio of the elastic ed to ep or e^{12}C yield. In the following paragraphs, we will for simplicity just refer to the ep scattering.

For elastic ep scattering, we have:

$$\left(\frac{d\sigma}{d\Omega}\right)_{ep} = \sigma_{Mott}\frac{E'_{ep}}{E}\left[\frac{G_E^2(Q_{ep}) + \tau G_M^2(Q_{ep})}{1+\tau} + 2\tau G_M^2(Q_{ep})\tan^2\left(\frac{\theta}{2}\right)\right], \quad (5)$$
$$\equiv \sigma_{Mott}\frac{E'_{ep}}{E}S_p(Q_{ep},\theta)$$

With the same target cuts and within the same scattering angle bin, the ratio of the charge-normalized yield is:

$$\frac{Y_{ed}(Q_{ed},\theta)}{Y_{ep}(Q_{ep},\theta)} = \frac{1+\frac{2E}{m_p}\sin^2\left(\frac{\theta}{2}\right)}{1+\frac{2E}{m_d}\sin^2\left(\frac{\theta}{2}\right)} \cdot \frac{S_d(Q_{ed},\theta)}{S_p(Q_{ep},\theta)} \cdot \frac{\rho_D}{\rho_H} \cdot \frac{R_{ed}}{R_{ep}} \tag{6}$$

where R_{ed} and R_{ep} are the radiative correction factors associated with the ed and the ep measurements. The relative charge can be determined to ≈0.1 %. The relative yields will be determined to about 0.2 % statistically. The target densities for H and D are each known to about 0.2 %, and the uncertainty in the relative density is about 0.3 %. Uncertainty in the relative radiative corrections will be of order 0.1 %. Uncertainties in corrections for the slight differences in kinematic factors - because the data point central and average values are different - are very small, as are uncertainties in the relative efficiencies between H and D, which were omitted from the equation. Thus, the relative cross sections measurements will be better than 1 %.

The existing world ^{12}C(e,e') data in the smaller Q kinematics of this experiment are good to roughly 1 % [37]. Since ^{12}C is a thin solid target rather than an extended target, there is an additional small solid angle correction and uncertainty. The use of both comparisons allows a further cross check of the data.

Deuteron ratio measurements

As a further check on the systematics of the data, we will also measure relative deuteron cross sections, and repeat all measurements with each of the spectrometers. For the relative measurements, one spectrometer measures the relative luminosity at one of the kinematic points, checking at the 0.1 % level, while the other spectrometer measures the deuterium (and hydrogen and carbon) absolute cross sections at all of the angles. The dominant angle dependent uncertainty is from the determination of Q (0.3 - 0.8 %); other relative uncertainties include statistics (0.2 %) solid angle (0.3 %), and radiative corrections (0.2 %).

Run plan and kinematics

We plan to start the experiment with a set of systematic and calibration checks, including beam energy measurements and current calibrations. Boiling tests are done automatically with the monitoring spectrometer during the data runs. Development and commissioning of the beam calorimeter will be done during facility development time prior to the experiment.

The kinematics and count rate estimate are listed in Table V, for a beam energy of $E = 0.857$ GeV. (This is a typical one-pass beam energy; the exact energy is not critical. If the energy is too high, it will be necessary to increase the momentum transfer of the lowest Q point.) The Table indicates that high data rates are possible; indeed, the difficulty is avoiding too high a data rate. With count rates of a few kHz in most kinematics, much of the experimental time is devoted to overhead, switching between targets and settings, and performing calibration measurements.

The run plan is to fix HRS-left at Kin-4 as a luminosity monitor, while HRS-right performs all measurements from Kin-1 to Kin-10. Thus, the deuteron form factors relative to those at

TABLE V: Table of kinematics and count rates, for $E = 0.857$ GeV.

	θ (degree)	Target	E' (GeV/c)	Q (GeV/c)	$I_{nominal}$ (μA)	Rate (Hz)	Time (Hours)
Kin-1_d	13.50	LD_2	0.8463	0.200	1.0	70k	0.50
Kin-1_p		LH_2	0.8359	0.199	1.0	180k	0.25
Kin-2_d	16.95	LD_2	0.8403	0.250	1.0	16k	0.50
Kin-2_p		LH_2	0.8243	0.248	1.0	67k	0.25
Kin-3_d	20.50	LD_2	0.8329	0.300	1.0	4k	0.50
Kin-3_p		LH_2	0.8101	0.297	1.0	28k	0.25
Kin-4_d	24.05	LD_2	0.8243	0.350	1.0	1.3k	0.50
Kin-4_p		LH_2	0.7940	0.344	1.0	13k	0.25
Kin-5_d	27.75	LD_2	0.8142	0.401	3.0	1.2k	0.50
Kin-5_p		LH_2	0.7755	0.391	1.0	6.6k	0.25
Kin-6_d	31.50	LD_2	0.8029	0.450	10.0	1.4k	0.50
Kin-6_p		LH_2	0.7553	0.437	1.0	3.5k	0.25
Kin-7_d	35.40	LD_2	0.7902	0.500	10.0	500	1.00
Kin-7_p		LH_2	0.7332	0.482	1.0	1.9k	0.25
Kin-8_d	43.65	LD_2	0.7609	0.600	50.0	350	1.50
Kin-8_p		LH_2	0.6842	0.569	1.0	600	0.75
Kin-9_d	52.70	LD_2	0.7263	0.700	50.0	61	3.0
Kin-9_p		LH_2	0.6302	0.652	1.0	200	1.0
Kin-10_d	62.90	LD_2	0.6863	0.800	50.0	11	4.0
Kin-10_p		LH_2	0.5724	0.731	1.0	85	1.0
Total beam on target: 2×17 **hours**							**34**

Kin-4 may be precisely determined. Then, the roles of the spectrometers will be reversed, and all measurements will be repeated. For each angle setting - and thus multiple times for Kin-4, we will measure spectra / cross sections for multiple targets, for calibrations of systematics and cross checks of cross sections. The targets include the following:

- ^{181}Ta foil,
- ^{12}C foil,
- optics target (multi-foil ^{12}C),
- ^{27}Al cryotarget empty cell,
- ^{2}H(e, e') target, and
- ^{1}H(e, e') target.

The comparison of the positions of the various elastic peaks on the focal plane provides a check of the scattering angle and spectrometer constant. The comparison of the y-target

TABLE VI: Estimated systematic uncertainties on absolute cross sections, hydrogen to deuterium ratio, and $A(Q)$ from the relative *ed* cross section angular distribution. A dash indicates the uncertainty is either negligible or not present. For the scattering angle uncertainty, we just use the largest value, for the lowest Q point.

systematic	uncertainty	$\frac{\delta\sigma_d}{\sigma_d\ abs}$	$\frac{\delta(Y_{ed}/Y_{ep})}{Y_{ed}/Y_{ep}}$	$\frac{\delta A(Q)}{A(Q)}$
Beam energy	0.02 %	0.1 %	-	-
Scattered electron energy	0.04 %	0.1 %	-	-
Scattered electron angle	0.3 mr	0.5 %	0.1 %	0.7 %
Beam charge Q	0.5 %	0.5 %	0.1 %	0.1 %
Target areal density	0.2 %	0.2 %	0.3 %	0.1 %
Target boiling	0.1 %	0.1 %	0.1 %	0.1 %
Solid angle $\Delta\Omega$	1.0 %	1.0 %	0.1 %	0.3 %
Radiative correction	1.0 %	1.0 %	0.1 %	0.1 %
$\epsilon_{detector}$	0.5 %	0.5 %	0.1 %	0.1 %
$\epsilon_{trigger}$	0.1 %	0.1 %	-	-
ϵ_{DAQ}	0.1 %	0.1 %	-	-
$\epsilon_{reconstruction}$	0.5 %	0.5 %	0.2 %	0.2 %
Total		1.8 %	0.4 %	0.8 %

spectra provides a check of the spectrometer pointing. The comparison of cross sections provides a check of the solid angle and absolute normalizations.

As indicated above, this run plan gives us several redundant ways to determine $A(Q)$. While we attempt to determine the absolute *ed* cross sections, which allows $A(Q)$ to be directly determined, we can also normalized the *ed* data to the *ep* or e^{12}C data at each point, or to the existing *ed* data or one of the theory calculations at one of the points. The second procedure then allows us to use much more precise relative cross sections. Finally, measurements are repeated with two different spectrometers, providing a stringent self-consistency constraint on the results.

In addition to performing these measurements at a standard one pass beam energy, we are requesting to repeat the measurement at a lower beam energy of 600 MeV. The main point is that consistent values of $A(Q)$ at two energies will add great confidence to the data. At lower beam energies, the sensitivity to the determination of Q is decreased, but the scattering increases, making the extended target effects and the magnetic corrections larger. We consider it sufficient to only repeat half of the Q settings for the second energy.

Systematic uncertainties discussed in the sections above are summarized in Table VI. These uncertainties all can be obtained in a carefully run experiment at present, once the beam calorimeter allows precise current measurements at low currents.

BEAM TIME REQUEST

The time request is summarized in Table VII. We request 4 days of beam time at a standard beam energy near 850 MeV, and 2 days of beam time at an energy of about 600

TABLE VII: Summary of beam time request.

Items	Time (hr) $E_e = 0.85$ GeV	Time (hr) $E_e = 0.60$ GeV
Beam on cryotarget	34.0	17.0
Beam on empty-target	8.0	4.0
Beam on ^{12}C targets	15.0	7.5
Beam on 181Ta target	2.0	1.0
Target movements	8.0	4.0
Spectrometer magnet and angle changes	8.0	4.0
Accesses to move spectrometer	6.0	6.0
Beam energy measurements (ARC+EP)	5.0	5.0
Beam charge calibration	1.0	1.0
Total	**83.0**	**46.5**

MeV, for this experiment. This request includes overhead time of target changes, magnets and spectrometer angle changes, beam energy measurement, beam charge calibration and a spectrometer optics check. Empty cell runs of 10 minutes at each setting are also included. The lower beam energy is the lowest at which it is currently considered standard to run beam to multiple halls. Hall accesses are needed to set up the spectrometers for runs near the minimum angles, 12.5°.

SUMMARY

We request six days to measure the *ed* elastic scattering $A(Q)$ structure function at low Q. The justification for this measurement is to improve upon the older data sets. At these Q, a description of $A(Q)$ is just out of the reach of current NNLO pionless effective field theories, but quite possible using chiral perturbation theory. Furthermore, conventional non-relativistic theories give roughly the average of the two data sets, while relativistic theories tend to agree either with the Mainz or with the Saclay data. Thus, the new measurements will better test the application of χPT to the deuteron, and will help improve understanding relativistic corrections at low Q. The measurements have potentially high impact on our understanding of the deuteron, and are of interest to numerous theoretical groups, yet require minimal beam time, and can be relatively easily done, with a careful experiment in Hall A.

[1] For a recent review, see Machleidt R and Slaus I *J. Phys. G* **27**, R69 (2001)
[2] Abbott D *et al. Phys. Rev. Lett.* **84**, 5053 (2000)
[3] Alexa L C *et al. Phys. Rev. Lett.* **82**, 1374 (1999)
[4] Abbott D *et al. Phys. Rev. Lett.* **82**, 1379 (1999)
[5] Abbott D *et al. Eur. Phys. J* A **7**, 421 (2000)

[6] Garçon M and Van Orden J W *Advances in Nucl. Phys.* **26**, 293 (2001)
[7] Sick I *Prog. Part. Nucl. Phys.* **47**, 245 (2001)
[8] Gilman R and Gross F, preprint nucl-th/0103020 and *J. Phys. G* **28**, R37 (2002)
[9] Simon G G *et al. Nucl. Phys.* A **364**, 285 (1981)
[10] Platchkov S *et al. Nucl. Phys.* A **510**, 740 (1990)
[11] Experimental limits on possible two photon exchange are discussed in Rekalo M P, Tomasi-Gustafsson E and Prout D *Phys. Rev.* C **60**, 042202 (1999)
[12] Gross F *Phys. Rev.* **136**, B140 (1965)
[13] Arnold R E, Carlson C E and Gross F *Phys. Rev.* C **21**, 1426 (1980)
[14] Donnelly T W and Raskin A S *Ann. Phys. (N.Y.)* **169**, 247 (1986)
[15] Berard R W *et al. Phys. Lett.* B **47**, 355 (1973)
[16] Benaksas D *et al. Phys. Rev.* **148**, 1327 (1966)
[17] Buchanan C D and Yearian R *Phys. Rev. Lett.* **15**, 303 (1965)
[18] Galster S *et al. Nucl. Phys.* B **32**, 221 (1971)
[19] Elias J E *et al. Phys. Rev.* **177**, 2075 (1969)
[20] Arnold R *et al. Phys. Rev. Lett.* **35**, 776 (1975)
[21] Phillips D R, Rupak R, and Savage M J PLB **473**, 209 (2000)
[22] Phillips D R, *Phys. Lett.* B **567**, 12 (2003)
[23] Mergell P, Meissner Ulf-G and Drechsel D *Nucl. Phys.* A **596**, 367 (1996)
[24] Phillips D R and Cohen T D *Nucl. Phys.* A **668**, 45 (2000)
[25] Walzl M and Meiβner U-G, *Phys. Lett.* B **513**, 37 (2001)
[26] Van Orden J W, Devine N and Gross F *Phys. Rev. Lett.* **75**, 4369 (1995)
[27] Forest J and Schiavilla R 2001 (to be published)
[28] Arenhövel H, Ritz F and Wilbois T *Phys. Rev.* C **61**, 034002 (2000)
[29] Allen T W, Klink W H and Polyzou W N PRC **63**, 034002 (2001)
[30] Carbonell J and Karmanov V A EPJA **6**, 9 (1999)
[31] Lev F M, Pace E and Salmé G PRC **62**, 064004 (2000)
[32] Phillips D R, Wallace S J, and Devine N K *Phys. Rev.* C **58**, 2261 (1998)
[33] Sick I and Trautmann D *Phys. Lett.* B **375**, 16 (1996); *Nucl. Phys.* A **637**, 559 (1998)
[34] Qattan I, *et al*, submitted to Phys. Rev. Lett.
[35] Ibrahim H, Ulmer P E, and Liyanage N, JLab-TN-02-32
[36] de Jager K, private communication
[37] Offermann E *et al. Phys. Rev.* C **44**, 1096 (1991)